Journal of Dental Research
2018, Vol. 97(12) 1355–1364

DOI: 10.1177/0022034518777746
journals.sagepub.com/home/jdr

Msx2 Prevents Stratified Squamous Epithelium Formation in the Enamel Organ

M. Nakatomi[1,2], H. Ida-Yonemochi[1], C. Nakatomi[3,4], K. Saito[1], S. Kenmotsu[1], R.L. Maas[5], and H. Ohshima[1]

Abstract

Tooth enamel is manufactured by the inner enamel epithelium of the multilayered enamel organ. *Msx2* loss-of-function mutation in a mouse model causes an abnormal accumulation of epithelial cells in the enamel organ, but the underlying mechanism by which *Msx2* regulates amelogenesis is poorly understood. We therefore performed detailed histological and molecular analyses of *Msx2* null mice. *Msx2* null ameloblasts and stratum intermedium (SI) cells differentiated normally in the early stages of amelogenesis. However, during subsequent developmental stages, the outer enamel epithelium (OEE) became highly proliferative and transformed into a keratinized stratified squamous epithelium that ectopically expressed stratified squamous epithelium markers, including Heat shock protein 25, Loricrin, and Keratin 10. Moreover, expression of hair follicle–specific keratin genes such as *Keratin 26* and *Keratin 73* was upregulated in the enamel organ of *Msx2* mutants. With the accumulation of keratin in the stellate reticulum (SR) region and subsequent odontogenic cyst formation, SI cells gradually lost the ability to differentiate, and the expression of Sox2 and Notch1 was downregulated, leading to ameloblast depolarization. As a consequence, the organization of the *Msx2* mutant enamel organ became disturbed and enamel failed to form in the normal location. Instead, there was ectopic mineralization that likely occurred within the SR. In summary, we show that during amelogenesis, *Msx2* executes a bipartite function, repressing the transformation of OEE into a keratinized stratified squamous epithelium while simultaneously promoting the development of a properly differentiated enamel organ competent for enamel formation.

Keywords: amelogenesis imperfecta, cell differentiation, growth and development, homeodomain proteins, keratin, tooth

Introduction

Tooth development proceeds through reciprocal interactions between the enamel organ and the dental mesenchyme (Tucker and Sharpe 2004; Jussila and Thesleff 2012), via sequential steps, including placodal, bud, cap, and bell stages (Nanci 2013). The enamel organ originally consists of the inner and outer enamel epithelium (IEE and OEE, respectively) and the stellate reticulum (SR). During the bell stage, the IEE gives rise to 2 cell layers, ameloblasts and stratum intermedium (SI) (Harada et al. 2006). Ameloblasts are responsible for enamel formation and undergo morphological and functional changes during amelogenesis, namely differentiation, secretory, transition, and maturation stages (Bartlett 2013). A key feature is that murine incisors grow continuously and thus provide an experimental advantage in that all developmental stages of amelogenesis can be examined in a sagittal section.

Transcription factors regulate downstream gene expression during odontogenesis. Among them, *Msx1, Msx2*, and *Msx3* in mammals are homologues of the *Drosophila muscle segment homeobox* (*msh*) gene (Alappat et al. 2003). *Msx2* is expressed during tooth development in dental epithelial tissues, including the enamel knot, OEE, SR, SI, IEE, preameloblasts, ameloblasts, Hertwig's epithelial root sheath (HERS), and the epithelial cell rest of Malassez (MacKenzie et al. 1992; Jernvall et al. 1998; Yamashiro et al. 2003; Bei et al. 2004; Aïoub et al. 2007; Molla et al. 2010). In vitro assays demonstrate that Msx2 interacts with CCAAT/enhancer-binding protein α to antagonize the transcriptional activation of *Amelogenin* (*Amel*) (Zhou et al. 2000; Xu et al. 2007).

[1]Division of Anatomy and Cell Biology of the Hard Tissue, Department of Tissue Regeneration and Reconstruction, Niigata University Graduate School of Medical and Dental Sciences, Niigata, Japan
[2]Division of Anatomy, Department of Health Promotion, Kyushu Dental University, Kitakyushu, Japan
[3]General Dentistry and Clinical Education Unit, Niigata University Medical and Dental Hospital, Niigata, Japan
[4]Division of Molecular Signaling and Biochemistry, Department of Health Promotion, Kyushu Dental University, Kitakyushu, Japan
[5]Division of Genetics, Department of Medicine, Brigham and Women's Hospital, Harvard Medical School, Boston, MA, USA

A supplemental appendix to this article is available online.

Corresponding Author:
H. Ohshima, Division of Anatomy and Cell Biology of the Hard Tissue, Department of Tissue Regeneration and Reconstruction, Niigata University Graduate School of Medical and Dental Sciences, 2-5274 Gakkocho-dori, Chuo-ku, Niigata 951-8514, Japan.
Email: histoman@dent.niigata-u.ac.jp

Previous studies have reported a variety of dental phenotypes in *Msx2* null mice (Bei et al. 2004; Aïoub et al. 2007; Molla et al. 2010; Babajko et al. 2014), especially an accumulation of epithelial cells in the enamel organ, reduced volume of the SR, and a deficit in enamel formation due to depolarized ameloblasts (Satokata et al. 2000). However, the developmental basis for this complex *Msx2* mutant odontogenic phenotype, including the origin of the hyperplastic epithelial cells that occupy the enamel organ, the etiology of the enamel dysplasia, and the cell fate of ameloblasts, remains to be elucidated.

To address these questions, we undertook detailed histological and molecular analyses of incisor and molar development in *Msx2* null mutant mice.

Materials and Methods

Mice

All animal experiments were conducted in compliance with a protocol reviewed by the Institutional Animal Care and Use Committee and approved by the president of Niigata University (permit number: Niigata Univ. Res. 315-1). Generation and genotyping of *Msx2* knockout mice ($Msx2^{-/-}$) on a C57BL/6J genetic background have been described previously (Satokata et al. 2000). Wild-type or heterozygous mutant ($Msx2^{+/-}$) littermates were used as controls. Mice were sacrificed at postnatal day (P) 1, 3, 5, and 9 and 7 wk, 10 wk, 20 wk, and 25 wk. At least 3 samples of wild-type and $Msx2^{-/-}$ were collected at each stage for histological analyses. Mice were fixed with perfusion fixation with 4% paraformaldehyde (PFA) solution. Dissected jaws were decalcified with Morse's solution. Wild-type embryos were dissected at embryonic day (E) 13.5, 15.5, and 17.5 and fixed with 4% PFA. Specimens were dehydrated through ethanol series, embedded in paraffin, and cut into 4-μm frontal or sagittal sections. Some sections were stained with hematoxylin and eosin (H&E).

In Situ Hybridization

Section and whole-mount in situ hybridizations were performed as described previously (Nakatomi et al. 2013). Digoxigenin-labeled RNA probes for *Ameloblastin* (*Ambn*) (Krebsbach et al. 1996), *Keratin 26* (*Krt26*), *Msx1* (Mackenzie et al. 1991), *Msx2* (Monaghan et al. 1991), and *Sonic hedgehog* (*Shh*) (Dassule and McMahon 1998) were prepared according to the manufacturer's protocol (Roche). Negative control sense probes did not yield significant staining (data not shown).

Immunohistochemistry

Immunohistochemical and terminal deoxynucleotidyltransferase-mediated dUTP nick end labeling (TUNEL) analyses were conducted as described elsewhere (Ida-Yonemochi et al. 2012). The antibodies used in this study are anti-Ambn (Uchida et al. 1997), Amel (Uchida et al. 1991), Desmoplakin, Enamelin (Enam) (Uchida et al. 1991), Heat shock protein 25 (Hsp25), Keratin 10 (K10), K14, K73, Loricrin, Notch1, Parathyroid hormone–related peptide (PTHrP) (Amizuka et al. 2000), and Sox2. Negative control experiments replacing primary antibodies with phosphate-buffered saline (PBS) did not yield significant staining (data not shown). More information on the antibodies is available in Appendix Table 1.

Reverse Transcription Polymerase Chain Reaction

The apical end region of the enamel epithelium of lower incisors (P9, P7w, and P20w) and facial skin (P9) of wild-type and $Msx2^{-/-}$ and palatal mucosa (P9) of wild-type were mechanically dissected for reverse transcription polymerase chain reaction (RT-PCR) analysis (n = 3 each of genotype). More information on the primer sequences is available in Appendix Table 2.

Transmission Electron Microscopy

Transmission electron microscopy (TEM) was carried out as previously described (Ohshima and Yoshida 1992), using an H-7100 transmission electron microscope (Hitachi High Corp.).

Cell Proliferation Assay

To examine cell proliferation activity, 5-bromo-2′-deoxyuridine (BrdU; Roche) dissolved in PBS was intraperitoneally injected into P9 pups at the concentration of 100 μg/g body weight 1 h before sacrifice (n = 3 each of genotype). Student's t test (2-tailed) was carried out to statistically compare BrdU numbers.

Electron Probe Microanalyzer

$Msx2^{+/-}$ and $Msx2^{-/-}$ littermates were dissected at P5 and P10w (n = 4 each) for electron probe microanalyzer (EPMA) analysis as described elsewhere (Osawa et al. 2007). Sagittally cut upper incisors and molars were analyzed by an EPMA (EPMA-8705; Shimadzu).

Micro–Computed Tomography

$Msx2^{+/-}$ and $Msx2^{-/-}$ littermates were dissected at P25w (n = 2 each) for micro–computed tomography (μ-CT) analysis as described elsewhere (Osawa et al. 2007), using Elescan (Nittetsu Elex) and a software program for 3-dimensional reconstruction (TRI/3D Bon; Ratoc System Engineering). A contrast stain using phophotungstic acid (Sigma-Aldrich) was performed as previously described (Metscher 2009).

Organ Culture

Lower first molar germs of wild-type and $Msx2^{-/-}$ (n = 4 each) were dissected at E15.5, cultured for 14 d, fixed, dehydrated, embedded, cut into 4-μm frontal sections, and stained with H&E.

More details are available in Appendix Materials and Methods.

Results

Normal Msx2 *Expression in the Outer Enamel Epithelium*

In situ hybridization revealed strong *Msx2* expression in the posterior end region of the lower incisor at P3 (Fig. 1A). In the upper incisor at P9, *Msx2* was extensively transcribed in preameloblasts at the early differentiation stage, transiently downregulated at the secretory stage, reboosted at the transition stage, and downregulated again at the maturation stage (Fig. 1B, E1–5). *Msx2* transcripts were detected in the SI, SR, and OEE through all stages of ameloblast differentiation (Fig. 1E1–5). Similar expression patterns were observed in molars at P9 (Appendix Fig. 1A, D1–4).

Ameloblast Depolarization and Cyst Formation in the Enamel Organ of Msx2$^{-/-}$

In *Msx2*$^{-/-}$ (hereafter referred to as mutant), ameloblasts became normally polarized at the differentiation and early secretory stages at P9 (Fig. 1G1–2). However, mutant ameloblasts gradually depolarized and their arrangement was disturbed in subsequent stages (Fig. 1G3–5), resulting in almost no enamel formation (Fig. 1D). Mutant ameloblasts were TUNEL negative in the early phase of amelogenesis, but the number of apoptotic ameloblasts in *Msx2*$^{-/-}$, where mutant ameloblasts lost their cellular polarity, was larger than that in wild-type (Appendix Fig. 2). Remarkably, the integrated layer containing the SI, SR, and OEE was abnormally thickened through all the stages (double-headed arrow in Fig. 1G1–5). Immunostaining for an SR marker PTHrP revealed that the SR did not properly form in *Msx2*$^{-/-}$ (Appendix Fig. 3). Moreover, an eosinophilic keratin-like structure was observed in the mutant enamel organ adjacent to ameloblasts (asterisk in Fig. 1G4–5; Appendix Fig. 4). Indeed, a large odontogenic cyst formed in the mutant enamel organ at P9 (Fig. 1H) and became enlarged and contained blood cells at P10w (Fig. 1I). This blood accumulation was clearly recognizable even through the maxillary bone at P10w (Appendix Fig. 5B). Semi-thin and TEM analyses confirmed the multilayered OEE and depolarized ameloblasts (Fig. 1J–L). In molar development at P5, the OEE continued with the dental lamina and became multilayered in *Msx2*$^{-/-}$ (Fig. 1N, P). The mutant SR region was occupied with an eosinophilic keratin-like structure (asterisk in Fig. 1N, P). Abnormally expanded OEE and odontogenic cyst formation in the enamel organ were also observed in mutant molars (Appendix Fig. 1C, F1–4, G, H). Due to loss of enamel, erupted molars suffered from severe attrition in *Msx2*$^{-/-}$ at P20w (Appendix Fig. 5D).

Expression of Ameloblast Differentiation Markers in Msx2$^{-/-}$

Hedgehog signaling is essential for the generation of ameloblasts (Seidel et al. 2010). *Shh* expression was not affected in the upper incisor of *Msx2*$^{-/-}$ at P9 (Fig. 2B; Appendix Fig. 6). Mutant ameloblasts expressed other differentiation markers such as Ambn, Amel, and Enam (Fig. 2D, F, H, J). The expression of *Msx1* was not significantly upregulated to compensate for decreased *Msx2* function in mutant ameloblasts (Fig. 2L). Similar results were obtained in mutant molars (Appendix Fig. 7B, D, F, H, J, L). Conventional RT-PCR analysis using complementary DNA (cDNA) derived from the enamel epithelium of the lower incisor at P20w confirmed relatively normal expression of other enamel organ-related genes *Amelotin* (*Amtn*), *Kallikrein 4* (*Klk4*), *Matrix metallopeptidase 20* (*Mmp20*), *Alkaline phosphatase* (*ALP*), *Notch1*, and *Sox2* in *Msx2*$^{-/-}$ (Appendix Fig. 7M).

SI Cells Dedifferentiate and Mislocalize in Msx2$^{-/-}$

SI cells in the incisor normally express Sox2 and Notch1 (Harada et al. 2006; Zhang et al. 2012). In the early phase of amelogenesis, Sox2 and Notch1 were similarly expressed, both to each other and between wild-type and *Msx2*$^{-/-}$ (arrow in Fig. 2M–P, S, T). However, immunoreactivity for Sox2 and Notch1 was partly downregulated in mutant SI cells at the secretory stage (asterisk in Fig. 2R, V), and some Sox2-positive cells mislocalized to more superficial layers (arrows in Fig. 2R). In addition, whereas desmosome marker Desmoplakin was expressed in both SI cells and ameloblasts in wild-type (arrows in Fig. 2W), its immunoreactivity decreased in *Msx2*$^{-/-}$ (asterisks in Fig. 2X).

Msx2$^{-/-}$ *OEE Is Highly Proliferative*

Next, a cell proliferation assay was performed using BrdU. In contrast to wild-type where BrdU-positive cells were rarely observed in the OEE (Fig. 3A–C; Appendix Fig. 8), a number of OEE cells were BrdU labeled in both incisors and molars in *Msx2*$^{-/-}$ (arrows in Fig. 3E, F; Appendix Fig. 8). The BrdU index in *Msx2*$^{-/-}$ was significantly higher than that in wild-type in both the buccal and lingual sides of molars and in the labial side of incisors (Fig. 3G).

Ectopic Epithelial Marker Expression in the Msx2$^{-/-}$ *Enamel Organ*

During amelogenesis, K14 was expressed in all the enamel organ cells in wild-type at P9 (Fig. 3H, K). K14 expression in *Msx2*$^{-/-}$ confirmed that the abnormally expanded enamel organ was filled with epithelium-derived cells (double-headed arrow in Fig. 3I, J, L). A keratinized stratified squamous epithelium consists of basal, spinous, and cornified layers from the basement membrane to the surface (Appendix Fig. 9A). Hsp25 is specifically expressed in the spinous layer, while Loricrin and K10 are markers for the cornified layer (Appendix Fig. 9C–E). Remarkably, Hsp25, Loricrin, and K10 were ectopically expressed within the mutant enamel organ outside of ameloblasts (arrow in Fig. 3N, O, S, T, X, Y, Q, V, AA; Appendix Fig.

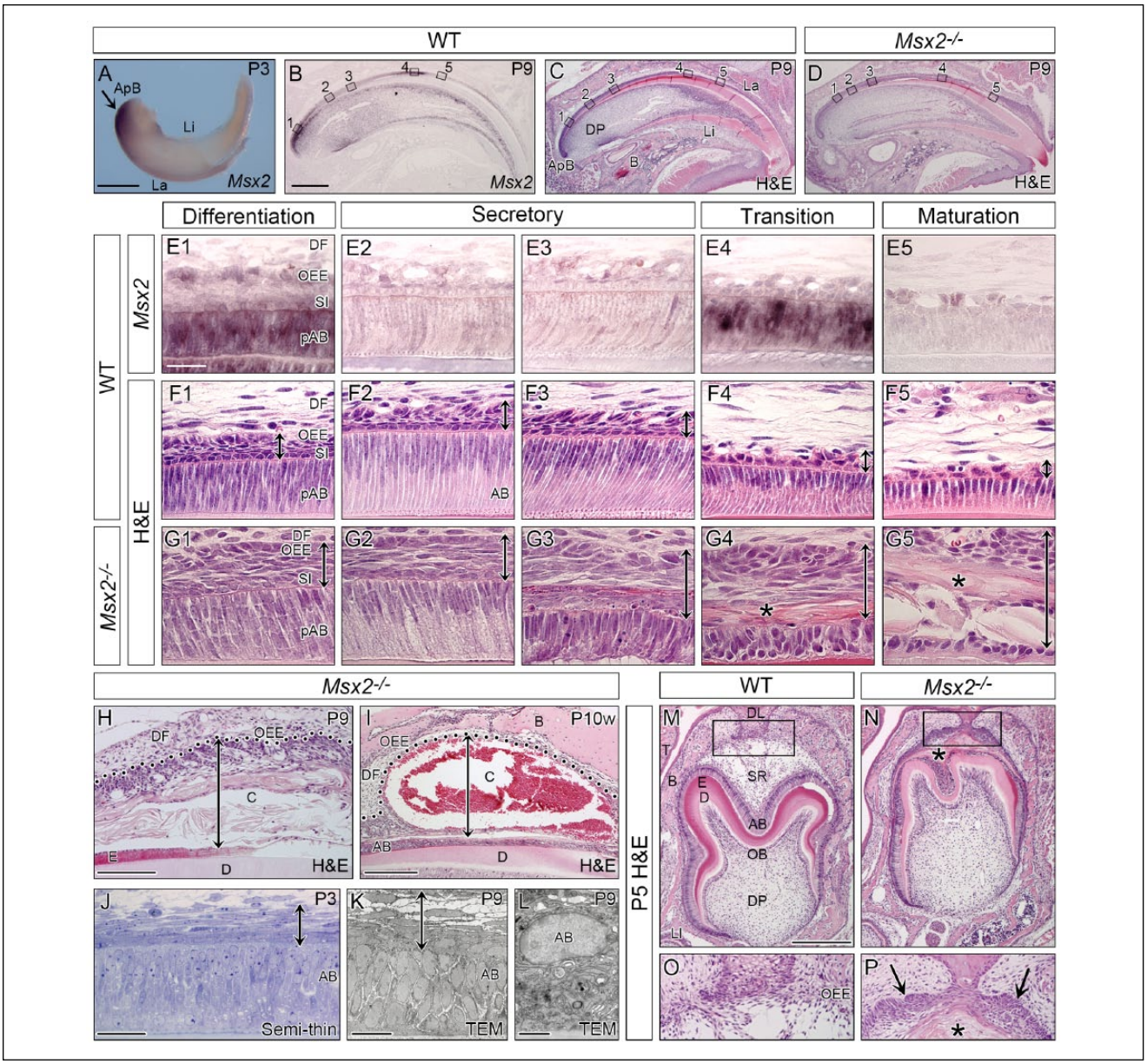

Figure 1. *Msx2* expression in WT and morphological phenotypes in mutant incisors and molars. Genotypes and stages are indicated. (**A–L**) Incisal edge side to right. (A) Whole-mount in situ hybridization of the lower incisor showing intense *Msx2* expression in the apical bud (ApB) region (arrow). (B–I) Section in situ hybridization of *Msx2* and hematoxylin and eosin (H&E)–stained sagittally sectioned upper incisors. (E–G) Magnified views of boxed areas in B to D. *Msx2* is expressed in the outer enamel epithelium (OEE), stratum intermedium (SI), and ameloblasts (AB) at the differentiation (E1) and transition (E4) stages but downregulated at the secretory (E2–3) and maturation (E5) stages. Mutant ameloblasts polarize normally at the differentiation and early secretory stages (G1–2) but depolarize abnormally afterward (G3–5). A stratified squamous epithelium forms ectopically in the mutant enamel organ (double-headed arrow in G1–5). An eosinophilic keratin-like structure is also observed (asterisk in G4–5). (H, I) An odontogenic cyst forms in the mutant enamel organ. Double-headed arrow indicates cyst thickness and dotted line demarcates epithelial-mesenchymal border. (J–L) Semi-thin analysis and transmission electron microscopy confirm the stratified squamous epithelium (double-headed arrow) and depolarized ameloblasts. (**M–P**) Frontally sectioned lower first molars. (O, P) Magnified views of boxed area in M and N. A stratified squamous epithelium ectopically forms and an eosinophilic keratin-like structure exists in the mutant enamel organ (asterisk and arrows in P). B, bone; C, cyst; D, dentin; DF, dental follicle; DL, dental lamina; DP, dental pulp; E, enamel; La, labial side; Li, lingual side; LI, lower incisor; OB, odontoblast; SR, stellate reticulum; T, tongue; WT, wild-type. Bars: 500 µm in A, 500 µm in B for B–D, 25 µm in E1 for E–G, 100 µm in H, 250 µm in I, 25 µm in J, 15 µm in K, 10 µm in L, and 250 µm in M for M and N.

9R, S, T) but were undetectable in wild-type. SI cells still remained at a differentiated state when a stratified squamous epithelium already formed in the mutant enamel organ at P9 (Appendix Fig. 10) and P10w (Appendix Fig. 11), suggesting that the OEE but not SI layer was responsible for the formation of the stratified squamous epithelium.

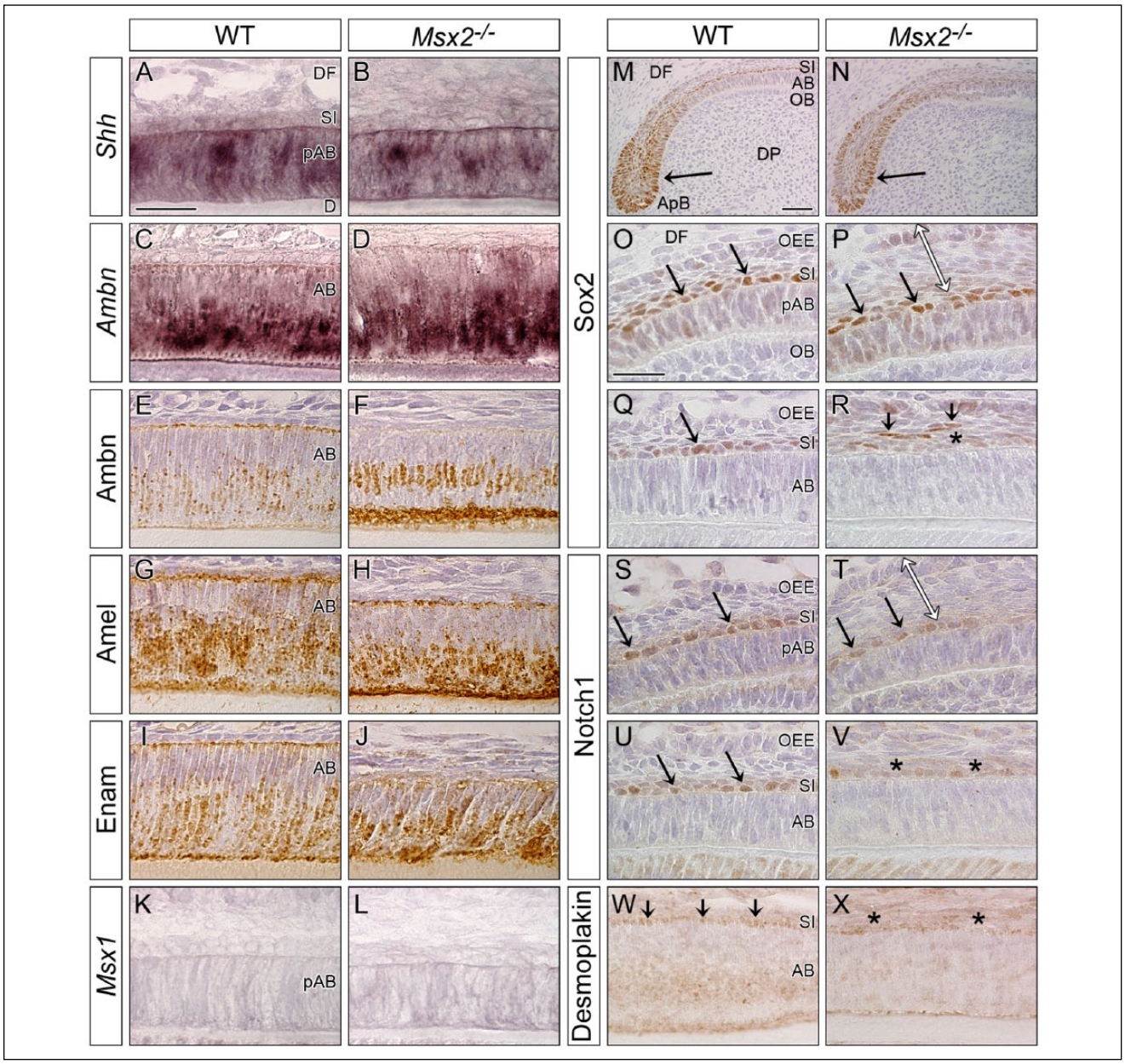

Figure 2. Ameloblasts and stratum intermedium cells initially differentiate in *Msx2*$^{-/-}$. Genotypes are indicated. Sagittally sectioned upper incisors at P9 (incisal edge side to right). (**A–D**, **K**, **L**) In situ hybridization. (**E–J**, **M–X**) Immunohistochemistry. (A, B) *Sonic hedgehog* (*Shh*) expression is detected in preameloblasts (pAB) in both genotypes. (C–J) Enamel proteins such as Ameloblastin (Ambn), Amelogenin (Amel), and Enamelin (Enam) are expressed in ameloblasts (AB) at the secretory stage in both genotypes. (K, L) *Msx1* is not significantly upregulated in *Msx2*$^{-/-}$. (M–V) Immunoreactivity for Sox2 and Notch1 is positive in the apical bud (ApB, arrow in M, N) and stratum intermedium (SI) cells (arrows in O, P, S, T) adjacent to pAB in both genotypes. Compared with wild-type (WT), SI cells neighboring AB partially lose immunoreactivity for Sox2 and Notch1 in *Msx2*$^{-/-}$ (asterisks in R, V), and some Sox2-positive cells detach from the original layer (arrows in R). Note that the outer enamel epithelium (OEE) is already expanded when SI cells are normally differentiated in *Msx2*$^{-/-}$ (double-headed arrow in P, T). (W, X) Compared with WT, desmosome marker Desmoplakin is partially attenuated between AB and SI cells of *Msx2*$^{-/-}$ (asterisks in X). D, dentin; DF, dental follicle; DP, dental pulp; OB, odontoblast. Bars: 25 μm in A for A–L, 50 μm in M for M and N, and 25 μm in O for O–X.

Upregulated Hair Keratin Expression in the Msx2$^{-/-}$ *Enamel Organ*

Keratins are categorized into epithelial and hair keratins, with the latter present in hair and nails (Kurokawa et al. 2011). The hair follicle consists of the inner root sheath (IRS) and the outer root sheath, each of which expresses characteristic hair keratins (Kurokawa et al. 2011). The type I keratin genes *Krt25, Krt26, Krt27*, and *Krt28* and the type II keratin genes *Krt71, Krt72*, and *Krt73* are specifically expressed in the IRS

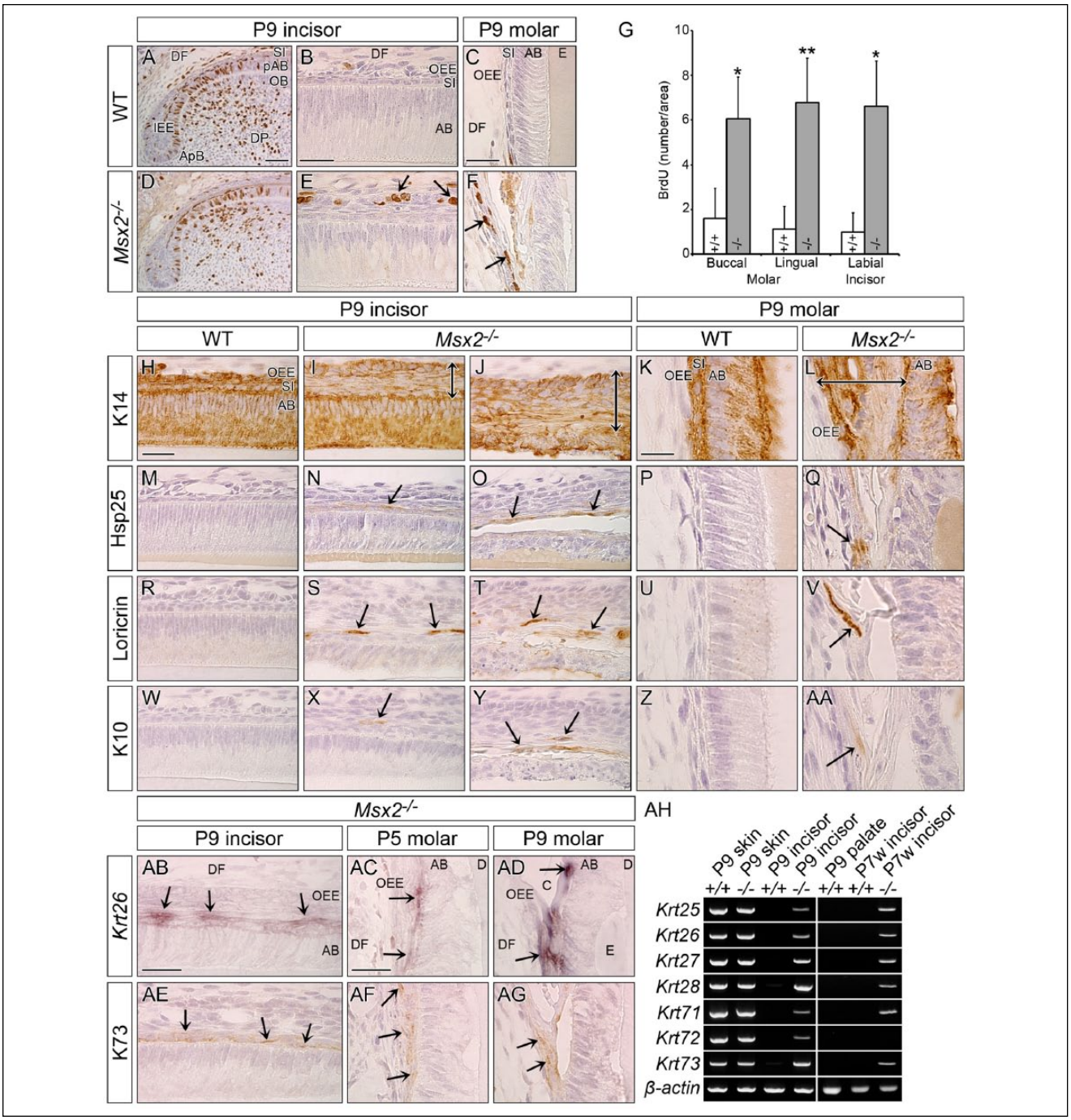

Figure 3. The mutant outer enamel epithelium is transformed to a highly proliferative keratinized stratified squamous epithelium. Genotypes and stages are indicated. (A, B, D, E, H–J, M–O, R–T, W–Y, AB, AE) Sagittally sectioned upper incisors (incisal edge side to right). (C, F, K, L, P, Q, U, V, Z, AA, AC, AD, AF, AG) Frontally sectioned lower first molars. (**A–F**) Immunohistochemical cell proliferation assay using BrdU 1 h labeling. Proliferating cells in the inner enamel epithelium (IEE) are strongly labeled with BrdU in both genotypes (A, D; see also Appendix Fig. 8). Compared with wild-type (WT), proliferative cells are ectopically observed in the outermost area of the mutant enamel organ (arrows in E, F). (**G**) Statistical analysis (Student's *t* test, 2-tailed) of cell proliferation in the outer enamel epithelium (OEE) of the buccal and lingual sides of molars and of the labial side of incisors reveals that the BrdU index is significantly higher in *Msx2*$^{-/-}$ than in WT (mean ± SD, $n = 3$). *$P < 0.05$. **$P < 0.01$. (**H–AA**) Immunohistochemistry for Keratin 14 (K14), Heat shock protein 25 (Hsp25), Loricrin, and Keratin 10 (K10). (**I**, **N**, **S**, **X**) are at the early secretory stage and (**J**, **O**, **T**, **Y**) show ameloblasts already depolarized. K14-immunoreactivity confirms that the abnormally expanded mutant enamel organ is an epithelial-derived tissue (double-headed arrow in I, J, L). Keratinized stratified squamous epithelium markers Hsp25, Loricrin, and K10 are ectopically expressed in the mutant enamel organ (arrows). (**AB–AG**) *Keratin 26* (*Krt26*) and Keratin 73 (K73) are upregulated in the mutant enamel organ (arrows), whereas no such expression is observed in WT (Appendix Fig. 13). (**AH**) Conventional reverse transcription polymerase chain reaction analysis using complementary DNA obtained from facial skin and palatal mucosa as a control tissue and the apical end of the labial epithelium in lower incisors at P9 and P7w. Hair follicle specific keratins are upregulated in the mutant tooth germ at both stages, except for *Krt72* at P7w. *β-actin* was used as an internal control. AB, ameloblast; ApB, apical bud; C, cyst; D, dentin; DF, dental follicle; DP, dental pulp; E, enamel; OB, odontoblast; pAB, preameloblast; SI, stratum intermedium. Bars: 50 μm in A for A and D, 25 μm in B for B and E, 25 μm in C for C and F, 25 μm in H for incisors, 15 μm in K for molars, 25 μm in AB for AB and AE, and 25 μm in AC for AC, AD, AF, and AG.

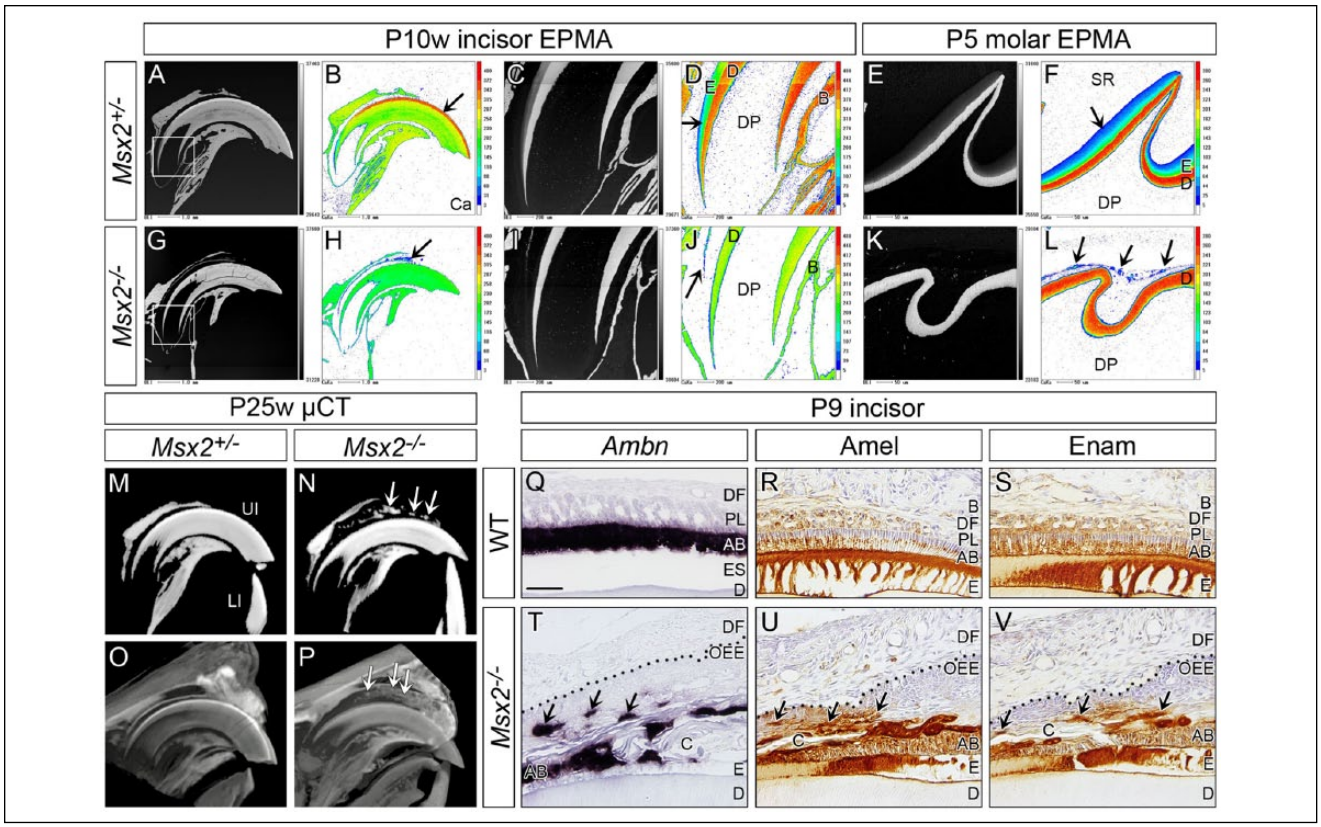

Figure 4. Ectopic amorphous mineralized structures are observed in the mutant enamel organ. Genotypes and stages are indicated. (**A–L**) Sagittal views obtained by electron probe microanalyzer (EPMA). (B, D, F, H, J, L) Calcium (Ca). (A–D, G–J) Upper incisors (incisal edge side to right). (C, D, I, J) Magnified views of boxed area in A and G. Compared to control, almost no enamel is on dentin and ectopic mineralized structures are observed between the incisor and surrounding bone in *Msx2*$^{-/-}$ (arrow in H, J). (E, F, K, L) Upper first molars (distal side to right). Similarly, almost no enamel forms and ectopic mineralized structures exist within the mutant enamel organ (arrows in L). Note that color scale is different depending on the magnification. In magnified views of controls (D, F), the color intensity of enamel is lower than that of dentin because enamel is immature and not fully mineralized at this stage. (**M–P**) Sagittal views of micro–computed tomography (µ-CT) analysis of upper incisors (incisal edge side to right). (M, N) Ectopic mineralized structures are detected between the incisor and surrounding bone in *Msx2*$^{-/-}$ (arrows in N). (O, P) A contrast stain using phosphotungstic acid reveals that such mineralized structures exist within the odontogenic cyst (arrows in P; see also Appendix Fig. 16). (**Q–V**) In situ hybridization of *Ameloblastin* (*Ambn*) and immunohistochemistry for Amelogenin (Amel) and Enamelin (Enam) of sagittally sectioned upper incisors (incisal edge side to right). Dotted line in T–V demarcates epithelial-mesenchymal border. Enamel protein-producing ameloblast-like cells localize to the cystic wall (arrows in T, U, V). AB, ameloblast; B, bone; C, cyst; D, dentin; DF, dental follicle; DP, dental pulp; E, enamel; ES, enamel space; LI, lower incisor; OEE, outer enamel epithelium; PL, papillary layer; SR, stellate reticulum; UI, upper incisor. Bar: 50 µm in Q for Q–V.

(Langbein et al. 2003; Langbein et al. 2006). *Msx2* and *Krt26* messenger RNA (mRNA) and K73 protein are coexpressed in whisker follicles of wild-type at P5 (Appendix Fig. 12B, D, E). Of interest, *Krt26* and K73 were upregulated in the mutant enamel organ, outside of ameloblasts in both incisors and molars (arrows in Fig. 3AB–AG), which were not detected in wild-type (Appendix Fig. 13). To further confirm these findings, conventional RT-PCR was carried out using cDNA derived from the skin, palatal mucosa, and the enamel epithelium of the lower incisor at P9 and P7w. *Krt25, Krt26, Krt27, Krt28, Krt71, Krt72*, and *Krt73* were upregulated in the mutant incisor at both P9 and P7w, except for *Krt72* at P7w (Fig. 3AH). Organ culture analysis using developing tooth germs dissected at E15.5 revealed that the abnormal multilayered enamel organ in *Msx2*$^{-/-}$ was the result of tooth germ intrinsic defects, rather than hormonal, metabolic, or other tooth germ extrinsic factors (Appendix Fig. 14).

Ectopic Amorphous Mineralized Structures in Msx2$^{-/-}$

EPMA analysis confirmed that enamel containing calcium, magnesium, and phosphate existed on the dentin in both incisors at P10w and molars at P5 in *Msx2*$^{+/-}$ controls (arrow in Fig. 4B, D, F; Appendix Fig. 15A–F). By contrast, no such obvious enamel matrix was seen in the corresponding region in *Msx2*$^{-/-}$ (Fig. 4H, J, L). Notably, however, amorphous mineralized structures were observed at a short distance from the dentin in both incisors and molars of *Msx2*$^{-/-}$ (arrow in Fig. 4H, J, L; Appendix Fig. 15G–L). Remarkably, µ-CT analysis confirmed these ectopic mineralized structures between the upper incisor and the surrounding bone in *Msx2*$^{-/-}$ at P25w (arrows in Fig. 4N). A contrast stain of µ-CT at P25w and histological analysis at P10w revealed that such mineralized structures existed within the odontogenic cyst (arrows in Fig. 4P;

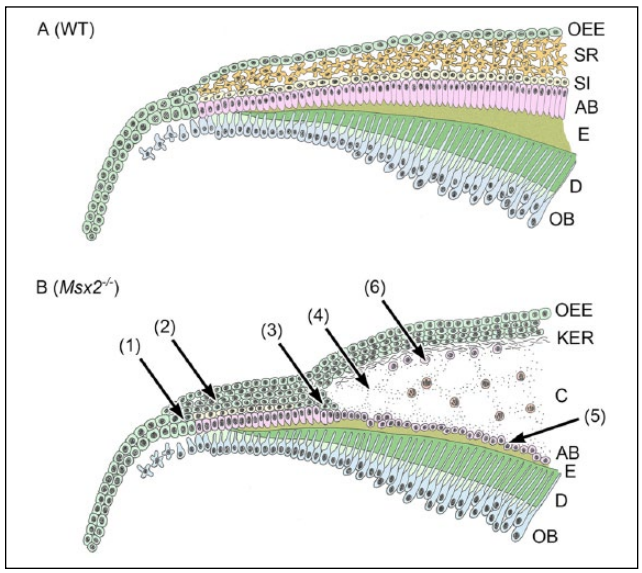

Figure 5. Schematic drawing of altered amelogenesis in *Msx2*$^{-/-}$. Two different contexts of the continuously growing rodent incisor and the molar with limited growth are integrated into one model. Mutant ameloblasts and SI cells normally differentiate in early amelogenesis (**1**). However, the OEE becomes highly proliferative and is transformed to a keratinized stratified squamous epithelium (**2**). As keratins accumulate in the enamel organ, SI cells dedifferentiate, leading to ameloblast depolarization (**3**). Subsequently, an odontogenic keratocyst forms (**4**). Note that depolarized ameloblasts survive and exist on a thin enamel matrix or directly on the dentin where such an enamel matrix is lost (**5**). Enamel protein-producing ameloblast-like cells and ectopic amorphous mineralized structures scatter in the cystic wall (**6**). AB, ameloblast; C, cyst; D, dentin, E, enamel; KER, keratin layer; OB, odontoblast; OEE, outer enamel epithelium; SI, stratum intermedium; SR, stellate reticulum.

Appendix Fig. 16). *Ambn*, Amel, and Enam were ectopically expressed in the lining epithelium of the odontogenic keratocyst of mutant upper incisors at P9 (arrows in Fig. 4T–V) and P10w (arrows in Appendix Fig. 17).

Discussion

It has been reported that the *Msx2*$^{-/-}$ enamel organ becomes abnormally filled with epithelial cells resulting in impaired enamel formation (Satokata et al. 2000), but the precise mechanism that underlies this phenotype has been obscure. The present study clearly reveals that *Msx2* deficiency transforms the OEE into a highly proliferative keratinized stratified squamous epithelium, expressing not only stratified squamous epithelial markers such as Hsp25, Loricrin, and K10 but also hair follicle–specific keratins, including *Krt26* and K73. Although ameloblasts and SI cells differentiate relatively normally in the early phase of amelogenesis in *Msx2*$^{-/-}$, these cells gradually lose their morphological features, and keratins that are normally expressed by a stratified squamous epithelium and by hair follicles ectopically accumulate in the enamel organ. These data indicate that *Msx2* function prevents the transformation of the OEE to a keratinized stratified squamous epithelium and that this inhibitory role is critical for the proper organization of the enamel organ and for enamel formation (summarized in Fig. 5). However, we cannot exclude the possibility that the SI is responsible for the abnormal structures in the enamel organ. To test this hypothesis, lineage tracing would be necessary, but currently there are no appropriate methods available.

Msx2 *Suppresses Transformation of the OEE in the Developing Tooth*

Although the dental epithelium originally derives from the oral epithelium, the tooth germ is a highly specified tissue, and thus a clear border appears between the dental lamina and the OEE (Fig. 1O; Appendix Fig. 9F). However, this border disappears in *Msx2*$^{-/-}$ and the stratified squamous epithelium extends continuously between the dental lamina and the enamel organ (Fig. 1P; Appendix Fig. 9P). Moreover, this ectopic stratified squamous epithelium becomes keratinized, resulting in the formation of an odontogenic keratocyst. Other rodent mutants such as whitish chalk-like teeth (*wct*) rats and *β1 integrin* conditional knockout mice also exhibit cyst formation in the enamel organ, but these cysts form in the ameloblast layer and are not keratinized (Osawa et al. 2007; Saito et al. 2015). Thus, cyst formation in the enamel organ can be categorized into 2 types, with or without keratinization, depending on whether the abnormality is intrinsic to the OEE or to ameloblasts, respectively. In addition, 7 hair follicle–specific keratins were remarkably upregulated in the mutant enamel organ, and all represent IRS-specific keratins. The relationship between *Msx2* and hair formation has been suggested by the occurrence of periodic hair loss and regrowth in *Msx2*$^{-/-}$ (Satokata et al. 2000; Ma et al. 2003). Another study revealed that *Krt33b* and *Krt86* were downregulated during nail development in *Msx2*$^{-/-}$ (Cai and Ma 2011). Taken together, *Msx2* appears to play a key role in regulating specific keratin expression positively or negatively in specific ectoderm-derived tissues. Interestingly, it has been proposed that hair follicle–specific keratins are involved in amelogenesis (Duverger et al. 2014), suggesting a possible role for *Msx2* in tightly regulating specific hair keratin expression during amelogenesis.

Dedifferentiation of SI Cells and Ameloblasts in Msx2$^{-/-}$

While *Msx2* function is not required for the initial differentiation of ameloblasts and SI cells, as keratinization progresses, SI cells gradually lose the expression of the differentiation markers Sox2 and Notch1. In addition, the expression of Desmoplakin in SI cells is downregulated in *Msx2*$^{-/-}$, suggesting that intercellular contact between SI cells and ameloblasts might be diminished. This inference agrees with the observation of decreased contact between ameloblasts based on TEM images and decreased expression of *Laminin5α3* in *Msx2*$^{-/-}$ (Bei et al. 2004). It has also been reported that adhesion at the ameloblast-SI cell interface via Nectin1, Nectin3, and PERP is essential for the maintenance of ameloblast cellular polarity and subsequent enamel formation (Barron et al. 2008; Yoshida

et al. 2010; Jheon et al. 2011). Therefore, we propose that SI dedifferentiation occurs initially due to a cell- or non-cell-autonomous requirement for *Msx2*, followed by ameloblast depolarization as a secondary consequence of disrupted connections between SI cells and ameloblasts. Another important issue is nutrients and oxygen supply. It could be possible that accumulated keratins and disappearance of the SR in the mutant enamel organ hinder transportation of nutrients and oxygen from blood capillaries located in the adjacent mesenchymal tissue, which may induce dedifferentiation of SI cells and subsequent depolarization and apoptosis of ameloblasts. Thus, our data indicate that *Msx2* is required to maintain the functional unit composed of OEE, SR, SI, and ameloblasts.

Ectopic Ameloblast-Like Cells and Mineralization in the Msx2$^{-/-}$ *Enamel Organ*

Notably, amorphous ectopic mineralized structures were observed by H&E staining, EPMA, and μ-CT between the tooth and the surrounding bone in both incisors and molars of *Msx2*$^{-/-}$. The localization of these mineralized structures coincides with ectopic ameloblast-like cells scattered throughout the cystic wall that express *Ambn*, Amel, and Enam. One potential mechanism for how these structures form in mutant enamel organs is that enamel matrix proteins secreted by ameloblast-like cells and mineral and ion leakage from capillary vessels might mix and ectopically mineralize. Although the origin of these ameloblast-like cells is unclear, the observation that depolarized ameloblasts detach and scatter throughout the cystic wall implies that *Msx2* deficiency does not interfere with ameloblast survival and that ameloblast depolarization does not impede the expression of enamel proteins. Further investigation is needed to elucidate the precise mechanism of ectopic mineralization in the mutant enamel organ.

In conclusion, our study identifies a novel role for *Msx2* in preventing the transformation of the OEE into a keratinized stratified squamous epithelium. Importantly, *Msx2* is also required for proper enamel organ differentiation and maintenance, and compromising this function accounts for an amelogenesis imperfecta phenotype in mice.

Author Contributions

M. Nakatomi, H. Ohshima, contributed to conception, design, data acquisition, analysis, and interpretation, drafted and critically revised manuscript; H. Ida-Yonemochi, C. Nakatomi, K. Saito, S. Kenmotsu, contributed to data acquisition, critically revised the manuscript; R.L. Maas, contributed to data acquisition, drafted and critically revised the manuscript. All authors gave final approval and agree to be accountable for all aspects of the work.

Acknowledgments

We are grateful to Dr. I. Satokata for providing *Msx2* mutant mice; Drs. R. Hill, P.H. Krebsbach, A.P. McMahon, and P.T. Sharpe for providing riboprobes; Drs. N. Amizuka and T. Uchida for providing antibodies; and Mr. M. Kobayashi and Ms. J. Pak for technical assistance. This work was supported by the National Institutes of Health to R.L.M. (R01DE011697) and by the Japan Society for the Promotion of Science KAKENHI (grants 25293371 and 17H04366 to H.O. and 25861741 to M.N.). The authors declare no potential conflicts of interest with respect to the authorship and/or publication of this article.

References

Aïoub M, Lézot F, Molla M, Castaneda B, Robert B, Goubin G, Néfussi JR, Berdal A. 2007. Msx2$^{-/-}$ transgenic mice develop compound amelogenesis imperfecta, dentinogenesis imperfecta and periodental osteopetrosis. Bone. 41(5):851–859.

Alappat S, Zhang ZY, Chen YP. 2003. Msx homeobox gene family and craniofacial development. Cell Res. 13(6):429–442.

Amizuka N, Fukushi-Irie M, Sasaki T, Oda K, Ozawa H. 2000. Inefficient function of the signal sequence of PTHrP for targeting into the secretory pathway. Biochm Biophys Res Commun. 273(2):621–629.

Babajko S, de La Dure-Molla M, Jedeon K, Berdal A. 2014. MSX2 in ameloblast cell fate and activity. Front Physiol. 5:510.

Barron MJ, Brookes SJ, Draper CE, Garrod D, Kirkham J, Shore RC, Dixon MJ. 2008. The cell adhesion molecule nectin-1 is critical for normal enamel formation in mice. Hum Mol Genet. 17(22):3509–3520.

Bartlett JD. 2013. Dental enamel development: proteinases and their enamel matrix substrates. ISRN Dent. 2013:684607.

Bei M, Stowell S, Maas R. 2004. Msx2 controls ameloblast terminal differentiation. Dev Dyn. 231(4):758–765.

Cai J, Ma L. 2011. Msx2 and Foxn1 regulate nail homeostasis. Genesis. 49(6):449–459.

Dassule HR, McMahon AP. 1998. Analysis of epithelial-mesenchymal interactions in the initial morphogenesis of the mammalian tooth. Dev Biol. 202(2):215–227.

Duverger O, Ohara T, Shaffer JR, Donahue D, Zerfas P, Dullnig A, Crecelius C, Beniash E, Marazita ML, Morasso MI. 2014. Hair keratin mutations in tooth enamel increase dental decay risk. J Clin Invest. 124(12):5219–5224.

Harada H, Ichimori Y, Yokohama-Tamaki T, Ohshima H, Kawano S, Katsube K, Wakisaka S. 2006. Stratum intermedium lineage diverges from ameloblast lineage via Notch signaling. Biochem Biophys Res Commun. 340(2):611–616.

Ida-Yonemochi H, Nakatomi M, Harada H, Takata H, Baba O, Ohshima H. 2012. Glucose uptake mediated by glucose transporter 1 is essential for early tooth morphogenesis and size determination of murine molars. Dev Biol. 363(1):52–61.

Jernvall J, Aberg T, Kettunen P, Keranen S, Thesleff I. 1998. The life history of an embryonic signaling center: BMP-4 induces p21 and is associated with apoptosis in the mouse tooth enamel knot. Development. 125(2):161–169.

Jheon AH, Mostowfi P, Snead ML, Ihrie RA, Sone E, Pramparo T, Attardi LD, Klein OD. 2011. PERP regulates enamel formation via effects on cell-cell adhesion and gene expression. J Cell Sci. 124(Pt 5):745–754.

Jussila M, Thesleff I. 2012. Signaling networks regulating tooth organogenesis and regeneration, and the specification of dental mesenchymal and epithelial cell lineages. Cold Spring Harb Perspect Biol. 4(4):a008425.

Krebsbach PH, Lee SK, Matsuki Y, Kozak CA, Yamada KM, Yamada Y. 1996. Full-length sequence, localization, and chromosomal mapping of ameloblastin: a novel tooth-specific gene. J Biol Chem. 271(8):4431–4435.

Kurokawa I, Takahashi K, Moll I, Moll R. 2011. Expression of keratins in cutaneous epithelial tumors and related disorders—distribution and clinical significance. Exp Dermatol. 20(3):217–228.

Langbein L, Rogers MA, Praetzel S, Winter H, Schweizer J. 2003. K6irs1, K6irs2, K6irs3, and K6irs4 represent the inner-root-sheath-specific type II epithelial keratins of the human hair follicle. J Invest Dermatol. 120(4):512–522.

Langbein L, Rogers MA, Praetzel-Wunder S, Helmke B, Schirmacher P, Schweizer J. 2006. K25 (K25irs1), K26 (K25irs2), K27 (K25irs3), and K28 (K25irs4) represent the type I inner root sheath keratins of the human hair follicle. J Invest Dermatol. 126(11):2377–2386.

Ma L, Liu J, Wu T, Plikus M, Jiang TX, Bi Q, Liu YH, Muller-Rover S, Peters H, Sundberg JP, et al. 2003. 'Cyclic alopecia' in Msx2 mutants: defects in hair cycling and hair shaft differentiation. Development. 130(2):379–389.

MacKenzie A, Ferguson MW, Sharpe PT. 1992. Expression patterns of the homeobox gene, Hox-8, in the mouse embryo suggest a role in specifying tooth initiation and shape. Development. 115(2):403–420.

MacKenzie A, Leeming GL, Jowett AK, Ferguson MW, Sharpe PT. 1991. The homeobox gene Hox 7.1 has specific regional and temporal expression patterns during early murine craniofacial embryogenesis, especially tooth development in vivo and in vitro. Development. 111(2):269–285.

Metscher BD. 2009. MicroCT for debelopmental biology: a versatile tool for high-contrast 3D imaging at histological resolutions. Dev Dyn. 238(3):632–640.

Molla M, Descroix V, Aioub M, Simon S, Castaneda B, Hotton D, Bolanos A, Simon Y, Lezot F, Goubin G, et al. 2010. Enamel protein regulation and dental and periodontal physiopathology in MSX2 mutant mice. Am J Pathol. 177(5):2516–2526.

Monaghan AP, Davidson DR, Sime C, Graham E, Baldock R, Bhattacharya SS, Hill RE. 1991. The Msh-like homeobox genes define domains in the developing vertebrate eye. Development. 112(4):1053–1061.

Nakatomi M, Ida-Yonemochi H, Ohshima H. 2013. Lymphoid enhancer-binding factor 1 expression precedes dentin sialophosphoprotein expression during rat odontoblast differentiation and regeneration. J Endod. 39(5):612–618.

Nanci A. 2013. Ten Cate's oral histology: development, structure, and function. 8th ed. St. Louis (MO): Elsevier.

Ohshima H, Yoshida S. 1992. The relationship between odontoblasts and pulp capillaries in the process of enamel- and cementum-related dentin formation in rat incisors. Cell Tissue Res. 268(1):51–63.

Osawa M, Kenmotsu S, Masuyama T, Taniguchi K, Uchida T, Saito C, Ohshima H. 2007. Rat wct mutation prevents differentiation of maturation-stage ameloblasts resulting in hypo-mineralization in incisor teeth. Histochem Cell Biol. 128(3):183–193.

Saito K, Fukumoto E, Yamada A, Yuasa K, Yoshizaki K, Iwamoto T, Saito M, Nakamura T, Fukumoto S. 2015. Interaction between fibronectin and beta1 integrin is essential for tooth development. PLoS One. 10(4):e0121667.

Satokata I, Ma L, Ohshima H, Bei M, Woo I, Nishizawa K, Maeda T, Takano Y, Uchiyama M, Heaney S, et al. 2000. Msx2 deficiency in mice causes pleiotropic defects in bone growth and ectodermal organ formation. Nat Genet. 24(4):391–395.

Seidel K, Ahn CP, Lyons D, Nee A, Ting K, Brownell I, Cao T, Carano RA, Curran T, Schober M, et al. 2010. Hedgehog signaling regulates the generation of ameloblast progenitors in the continuously growing mouse incisor. Development. 137(22):3753–3761.

Tucker A, Sharpe P. 2004. The cutting-edge of mammalian development; how the embryo makes teeth. Nat Rev Genet. 5(7):499–508.

Uchida T, Murakami C, Dohi N, Wakida K, Satoda T, Takahashi O. 1997. Synthesis, secretion, degradation, and fate of ameloblastin during the matrix formation stage of the rat incisor as shown by immunocytochemistry and immunochemistry using region-specific antibodies. J Histochem Cytochem. 45(10):1329–1340.

Uchida T, Tanabe T, Fukae M, Shimizu M, Yamada M, Miake K, Kobayashi S. 1991. Immunochemical and immunohistochemical studies, using antisera against porcine 25 kDa amelogenin, 89 kDa enamelin and the 13-17 kDa nonamelogenins, on immature enamel of the pig and rat. Histochemistry. 96(2):129–138.

Xu Y, Zhou YL, Erickson RL, Macdougald OA, Snead ML. 2007. Physical dissection of the CCAAT/enhancer-binding protein alpha in regulating the mouse amelogenin gene. Biochem Biophys Res Commun. 354(1):56–61.

Yamashiro T, Tummers M, Thesleff I. 2003. Expression of bone morphogenetic proteins and Msx genes during root formation. J Dent Res. 82(3):172–176.

Yoshida T, Miyoshi J, Takai Y, Thesleff I. 2010. Cooperation of nectin-1 and nectin-3 is required for normal ameloblast function and crown shape development in mouse teeth. Dev Dyn. 239(10):2558–2569.

Zhang L, Yuan G, Liu H, Lin H, Wan C, Chen Z. 2012. Expression pattern of Sox2 during mouse tooth development. Gene Expr Patterns. 12(7–8):273–281.

Zhou YL, Lei Y, Snead ML. 2000. Functional antagonism between Msx2 and CCAAT/enhancer-binding protein alpha in regulating the mouse amelogenin gene expression is mediated by protein-protein interaction. J Biol Chem. 275(37):29066–29075.